Asian Journal of Chemistry; Vol. 33, No. 9 (2021), 2127-2134

ASIAN JOURNAL OF CHEMISTRY

https://doi.org/10.14233/ajchem.2021.23306

Characterization, Molecular Docking, Antimicrobial and Anticancer Studies on 5-Bromo salicylaldehyde-furan-2-yl-methanamine Condensed Schiff Base Rare Earth Metal Complexes

B. PREETHI[1], R. JAYAPRAKASH[2], S. KUTTI RANI[1,*] and N. VIJAYAKUMAR[3]

[1]Department of Chemistry, B.S. Abdur Rahman Crescent Institute of Science and Technology, Vandalur, Chennai-600048, India
[2]Department of Chemistry, School of Arts and Science, Aarupadai Veedu Institute of Technology Campus, Vinayaka Mission's Research Foundation (Deemed to be University), Chennai-603104, India
[3]Department of Biochemistry and Biotechnology, Faculty of Science, Annamalai University, Chidambaram-608002, India

*Corresponding author: E-mail: skrani@crescent.education

Received: 14 May 2021; *Accepted*: 27 June 2021; *Published online*: 20 August 2021; AJC-20474

This work described the synthesis and characterization of 1-(furan-2-yl) methanamine condensed with 5-bromo-2-hydroxybenzaldehyde Schiff base rare earth metal (Ln^{3+}, Pr^{3+}, Nd^{3+}, Sm^{3+} and Eu^{3+}) complexes. They were characterized using relevant spectral techniques and docked against microbial target proteins (1H9Z, 3ZBO) theoretically. The experimental antibacterial and anticancer activities (HeLa, MCF7) of these metal complexes were investigated for biological efficacy. Out of five metal complexes, Pr^{3+} complex exposed good biological efficacy result in both assays.

Keywords: Schiff base, Rare-earth metals, Antibacterial activity, Anticancer activity.

INTRODUCTION

The organometallic chemistry of rare earth metals research is a growing field for various applications [1,2]. Particularly, the Schiff bases coordinated with lanthanides have been received broad interest in the field of coordination chemistry and medicinal research [3]. Also, the Schiff base coordinated lanthanide complexes have exhibited the significant antifungal, antibacterial and regulating the plant growth characters [4,5]. This different metal complexes with Schiff bases research increases due to –CH=N- like donor atoms, stability and their mechanism in biological effectiveness [6-8]. In addition, the developing medicinal and software based computational techniques are also exposed with great interest to reduce the time and waste of chemicals in research fields [9-11]. Also, they are providing basic structural properties and their reactivity in biological studies. Similarly, the antimicrobial studies using agar broth medium and cancer studies on specific cell lines are widely used to measure the resistivity of the synthesized compounds [12,13]. Based on the literature, this work reports the synthesis, characterization the five rare earth metal(III) (*viz*. Ln^{3+}, Pr^{3+}, Nd^{3+}, Sm^{3+} and Eu^{3+}) complexes from 1-(furan-2-yl)methanamine condensed with 5-bromo-2-hydroxybenzaldehyde Schiff base (5BSFASB). The derived complexes were characterized using UV-visible, FTIR, NMR and mass spectral techniques wherever required. After the confirmation, the compounds were carried for theoretical docking studies against microbial proteins such as 1H9Z and 3ZBO using online patchdock for ligand and offline iGEMDOCK for all compounds [14-16]. To compare the theoretical outcomes, experimental antimicrobial activity was investigated by ager well diffusion method. After the microbial screening, best molecule was carried for the further anticancer activity or cytotoxicity on HeLa and MCF7 cells by MTT assay [17]. The experimental biological outcomes were compared with the theoretical docking outputs.

EXPERIMENTAL

The chemicals such as rare earth metal(III) hexanitrate salts (La^{3+} = Ln^{3+}, Pr^{3+}, Nd^{3+}, Sm^{3+} and Eu^{3+}) were purchased from SRL Chemicals, India. This work used AR grade solvents for the experimental preparations and were used after purifications. The UV-visible spectra of the ligand and the complexes were analyzed using LS25-UV Perkin-Elmer. Vibrational FT-IR spectra were recorded in JASCO FTIR-6300 through KBr

pellets. Both ^{1}H & ^{13}C NMR spectra of the ligand and complexes were recorded in Bruker NMR-400 spectrometer in DMSO-d_6. The prepared ligand and rare metal complexes were recorded by Shimadzu LC-MS 2020 Mass spectra. Colorimetric MTT assay was measured by ELISA plate reader for the inhibition study. Proteins PDB files of 1H9Z, 3ZBO targets were obtained from RCSB data bank (https://www.rcsb.org/pdb/home/home.do). Offline docking conducted using Rosmol and java based iGEMDOCK software. Antimicrobial pathogens such as *E. coli* ATCC 25922, *Klebsiella pneumoniae* ATCC 35657, *Acinetobacter baumannii* ATCC 19606, *Proteus mirabilis* ATCC 635659, *Pseudomonas aeruginosa* ATCC 27853, *Salmonella typhimurium* ATCC 14028, *Methicillin* resistant *Staphylococcus aureus* ATCC 100698, *Shigellaboydii* MTCC 11947 and *Staphylococcus aureus* MTCC 1430, were purchased from American type culture collection. The human breast adenocarcinoma cancer (MCF7) and human cervical cancer (HeLa) cell lines were received from the National Centre for Cell Sciences, Pune, India. The (3-(4,5-dimethylthiazol-2-yl)-2,5-diphenyltetrazolium bromide, a yellow tetrazole-MTT was purchased from Sigma-Aldrich, India.

Synthesis of 5-bromo-2-hydroxy-benzaldehyde Schiff base (5BSFASB) and its rare metal complexes: A methanolic solution of 2-furfuryl amine (50 mmol, 4.85 g) and 5-bromo salicylaldehyde (50 mmol, 9.5 g) were refluxed in methanol for 1 h. 60:40 ethyl acetate and hexane TLC system was used to monitor the chemical reaction. After the completion of the reaction yellow solid (5BSFASB) was isolated and crystallized in 1:1 acetonitrile-methanol. The 1 mmol of filtered and dried pure solid crystals were treated with 0.5 mmol of different lanthanide(III) nitrate salts separately in methanol solvent [18]. After 3 h, the obtained clear yellow solution was maintained for 1 h at the same temperature. It was cooled to room temperature. The filtered crystalline solids were dried in desiccators over anhydrous calcium chloride.

2-(Furan-2-ylmethyl)imino]methyl}-4-bromo phenol (5BSFASB): Light yellow crystals, yield: 80%, m.p.: 155-165 ºC. ^{1}H NMR (500 MHz, DMSO-d_6) δ 13.23 (s, 1H), 8.65 (s, 1H), 7.73 (d, J = 5 Hz, 1H), 7.65 (d, J = 5 Hz, 1H), 7.49 (dd, 1H), 6.88 (d, J = 10 Hz, 1H), 6.46 (t, J = 5 Hz, 1H), 6.40 (d, J = 5 Hz, 1H), 4.81 (s, 2H). ^{13}C NMR (125 MHz, DMSO-d_6): 166, 160, 151, 138, 133, 130, 120, 119, 111, 109, 108, 54. *m/z* $(M+H)^+$: 281.83.

5BSFASB-La(III) (a): Light yellowish brown solid, yield: 70%, m.p.: 205-210 ºC. ^{1}H NMR (500 MHz, DMSO-d_6) δ ppm: 4.66 (s, 2H), 6.12 (br s, 1H), 6.27-6.37 (m, 1H), 6.82 (br d, J = 7.48 Hz, 1H) 7.41 (br d, J = 7.21 Hz, 1H) 7.48 (s, 1H), 7.75 (s, 1H) 8.10 (s, 1H). *m/z* $(M+H)^+$: 841.88.

5BSFASB-Pr(III) (b): Light yellowish green solid, yield: 60%, m.p.: 180-195 ºC. ^{1}H NMR (500 MHz, DMSO-d_6) δ ppm: 2.28 (br d, J = 12.45 Hz, 1H), 2.52 (br d, J = 12.45 Hz, 1H), 4.54 (br d, J = 12.45 Hz, 1H), 4.78 (br d, J = 12.45 Hz, 1H), 6.07-6.17 (m, 2H), 6.27-6.37 (m, 2H), 6.97 (br d, J = 7.32 Hz, 2H), 7.48 (s, 2H), 7.60 (br d, J = 6.89 Hz, 2H) 7.72 (s, 2H), 8.48 (s, 2H). *m/z* $(M+H)^+$: 844.03.

5BSFASB-Nd(III) (c): Light yellowish solid, yield: 60%, m.p.: 200-210 °C, ^{1}H NMR (500 MHz, DMSO-d_6) δ ppm 4.66 (s, 2 H) 6.12 (br s, 1 H) 6.27-6.37 (m, 1 H) 6.82 (br d, J = 7.48 Hz, 1 H) 7.41 (br d, J = 7.21 Hz, 1 H) 7.48 (s, 1 H) 7.75 (s, 1 H) 8.10 (s, 1 H). *m/z* $(M+H)^+$- 846.88.

5BSFASB-Sm(III) (d): Light yellowish solid, yield: 65%, m.p.: 190-205 ºC ^{1}H NMR (500 MHz, DMSO-d_6) δ ppm 4.66 (s, 2H), 6.12 (br s, 1H), 6.27-6.37 (m, 1 H) 6.82 (br d, J = 7.48 Hz, 1H), 7.41 (br d, J = 7.21 Hz, 1H), 7.48 (s, 1H) 7.75 (s, 1H) 8.10 (s, 1H). *m/z* $(M+H)^+$: 856.89.

5BSFASB-Eu (III) (e): Light yellowish solid, yield: 60%, m.p.: 220-215 ºC. ^{1}H NMR (500 MHz, DMSO-d_6) δ ppm: 4.66 (s, 4H), 4.84 (s, 4H), 6.12 (br s, 2H), 6.32 (s, 1H), 6.33 (d, J = 5.49 Hz, 1H), 6.83 (s, 1H), 7.36 (s, 1H), 7.48 (s, 2H), 7.72 (s, 1H), 7.78 (s, 1H), 8.10 (s, 2H). *m/z* $(M+H)^+$: 855.89.

The proposed structure of the rare earth metal(III) complexes are shown in Fig. 1.

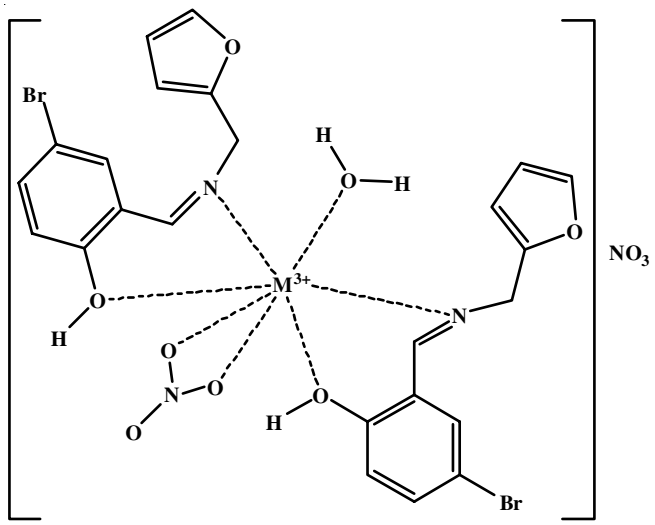

M^{3+} = Ln^{3+} (a), Pr^{3+} (b), Nd^{3+} (c), Sm^{3+} (d) and Eu^{3+} (e)

Fig. 1. Structure of lanthanide complexes (**a-e**)

Docking study: The downloaded protein PDB: 1H9Z (human serum albumin transport protein which is easily bind with all drugs), 3ZBO (heat-like repeat DNA glycosylases) were used for docking using iGEMDOCK software. Each converted pdb structures of ligand and metal complexes were uploaded for the interaction analysis calculation. After the simulation, the binding energy was calculated for the ligand and complexes to correlate with experimental cancer and antimicrobial activities.

Antimicrobial study: As per the guidance of the National Committee for Clinical Laboratories Standard and based on the references, broth dilution method conducted for the test samples with modification of the dilution medium and the specific concentration effect on the bacterial growth was measured in term of zone of inhibition of the pathogens [19,20]. The synthesized ligand 5BSFASB and its rare metal(III) complexes (**a-e**) were carried for MIC study using 250 ppm concentration. The antibacterial nature of the complex on solid agar was determined.

Cytotoxicity assay: MCF7 and HeLa 100 cells were obtained from Pune-NCCS and were cultured at 37 ºC in a

moistened with 5% CO_2 containing atmosphere. The selected and cultured HeLa and MCF7 cells were seeded into 96 well plates for 48 h. Both cells were treated with a serially diluted highly active metal complex. A known anticancer agent 5-fluoro uracil (100 mM) was used as control and treated with both cancer cells. The plates were cultured for 48-72 h after the treatment with control and active metal complexes [21]. MTT (5 mg/mL) was prepared and 100 µL was added in each well. After 4 h incubation, formed purple colour formazone was dissolved in 100 µL of DMSO, which was measured at 620 nm using ELISA plate reader. The OD value used to measure the inhibition through the following formula:

$$\text{Cell viability } (\%) = \frac{(A_{\text{treatment}} - A_{\text{blank}})}{(A_{\text{control}} - A_{\text{blank}})} \times 100$$

RESULTS AND DISCUSSION

Electronic spectra: The electronic absorption spectral data of the furan based metal complexes in ethanol are recorded to observe the changes when treated with metal nitrates. Absorption spectra of ligand 5-bromo salicylaldehyde furyl methanamine condensed schiff base (5BSFASB) and their rare metal(III) complexes were recorded in ethanol between the range of 200 and 900 nm. The absorption spectra in ethanol exhibited the characteristic peaks between 222 and 400 nm. The Schiff base ligand 5BSFASB displayed π→π* band due to the aromatic ring at 225 nm at higher energy. Also, it exposed the bands at 257 and 327 nm for the n→π*, π→π* transitions (lower energy) due to lone pair electrons in p orbital of azomethine N atom. These absorption bands were coincidence with reported spectral data [22]. Owed to the like structure of the prepared rare metal complexes, five rare earth metal complexes displayed significant peaks (Fig. 2) with slight deviation in absorption intensity [23]. The comparison of absorption band regions between ligand and metal complexes (**a-e**) are presented in Table-1. The results revealed that the slight bathochromic shift in all the metal-complexes which is due to more dipolar excited states. Owing to the interaction of solvent ethanol and water in complexes, the shift was slightly decreased from 225 and 327 nm.

TABLE-1
ABSORPTION SPECTRA VALUE OF FBS COMPLEXES

	5BSFASB	La^{3+} (a)	Pr^{3+} (b)	Nd^{3+} (c)	Sm^{3+} (d)	Eu^{3+} (e)
Wavelength (nm)	225	223	216	220	219	215
	327	323	325	323	324	323

FTIR studies: In Schiff base ligand 5BSFASB, infrared spectra displayed the significant peaks for hydroxyl (-OH) and azomethine group (-CH=N-) peaks at 2630 cm^{-1} and 1627 cm^{-1}, respectively. The band appeared at 1366 cm^{-1} in ligand is assigned to ν(CO) stretching frequency. Thus, the IR spectra of the ligands are found to be in good agreement with their respective structural features. In addition, broad peak exists between 3200 and 2800 cm^{-1} for 5BSFASB–OH, the -NH peaks coincidence with reported frequencies [24]. The FTIR spectra of the complexes **a-e** exposed the region for 5BSFASB La(III), Pr(III), Nd(III), Sm(III) and Eu(III) complexes exhibited the broad peak with a high intensity, which represents the weak hydrogen bonds [25]. This band is associated with the existence of water of the derived complexes, which is the characteristic band for the OH stretching vibrations. But in La(III) complex, this peak is marginally differed. All the rare metal(III) complexes exhibited the characteristic M-O bond at the frequencies in cm^{-1} such as 430 (La-O), 432 (Pr-O), 433 (Nd-O), 435 (Sm-O) and 438 (Eu-O). In addition to this change in frequency, rare metal(III) complexes exposed the deviation of azomethine frequency from 1627 to 1590 cm^{-1} [26]. This deviation confirmed that the coordination of imine with nitrate salts of rare earth metal(III). The corresponding FTIR of the ligand and its rare earth metal(III) complexes **(a-e)** are shown in Fig. 3.

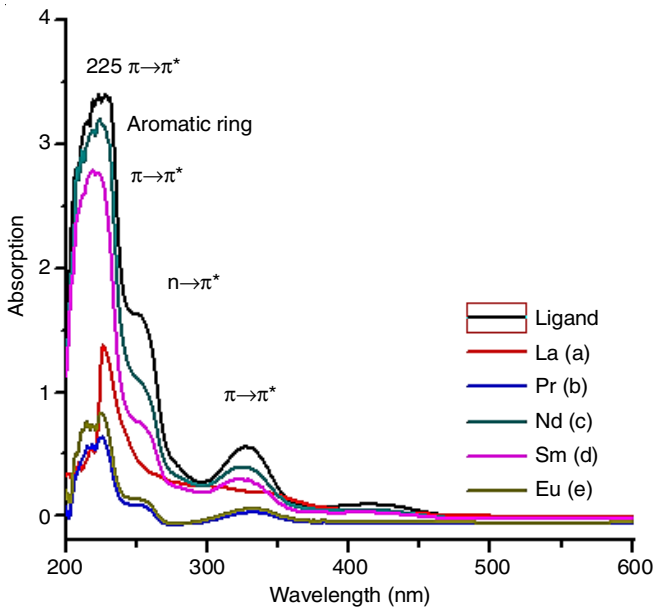

Fig. 2. Electronic spectra of ligand

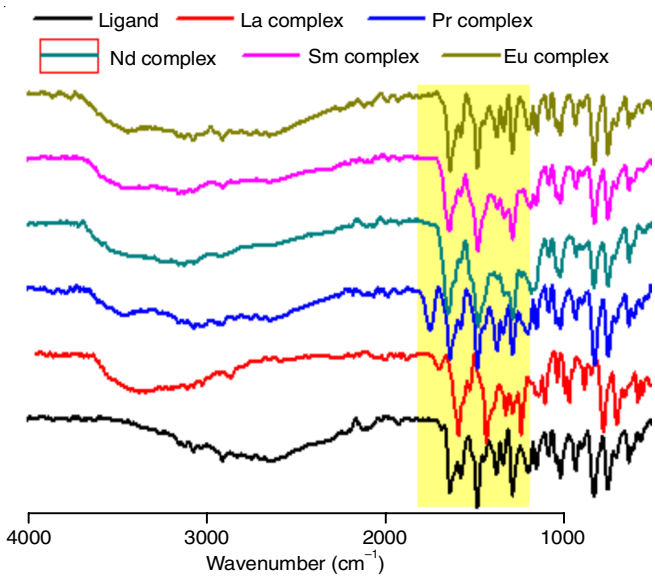

Fig. 3. FTIR spectra of 5BSFASB and its metal complexes

^{1}H & ^{13}C NMR studies: After the basic functional group changes, the ligand was characterized by both ^{1}H & ^{13}C NMR spectral studies. Ligand 5BSFASB exhibited the ^{1}H NMR peaks at δ13.23 ppm (-OH), 8.65 (-CH=N-), 4.81 (-CH_2-) and rest of the peaks confirmed the aromatic ring of the ligand. ^{13}C NMR of 5BSFASB ligand has the carbon peaks at 166 ppm (C-OH), 160 ppm for (-CH=N-) and remaining peaks between 6.0 and 7.5 ppm confirmed the aromatic carbons of the condensed molecule. But, hydroxyl group peaks were absent in metal complexes. In addition, imine peak slightly shifted from 8.65 to 8.1-8.3 ppm, which confirmed the coordination of metals with imine nitrogen. In addition, all the rare earth metal(III) complexes are similar structure hence some peaks commonly exist in spectra. But these complexes are differed in water of hydration whereas in samarium(III) complex, the water of hydration is higher than other complexes. Imine proton non-involvement in coordination was confirmed from the imine proton dislocation in spectra of all compounds. The reported values are coincidence with the reported values [27].

Mass studies: The complex molecular nature was identified by mass spectrum and correlated with calculated molecular weight for the structure. The mass spectra of 5BSFASB complexes showed the base peaks of *m/z* (M+H) 841.88, 844.03, 846.88, 856.89, 855.89 and 847.89, respectively. The base peak of La(III), Pr(III), Nd(III), Sm(III) and Eu(III) complexes molecular ion peaks confirmed the 1:2 stoichiometry of ligand, one nitrate and one water molecules in coordination sphere with one nitrate counter ion which was coincidence with reported value [28]. Moreover, the complex may have the common molecular formula of lanthanides $(C_{12}H_{10}NO_2Br)_2(NO_3)(H_2O)]$-$NO_3$ and the ligand is a bidentate in nature.

Theoretical docking: The characterized compounds were carried for the computational docking to measure the inhibition tendency of the target proteins like drug transporting protein (1H9Z) and common living organism protein (3ZBO). The docking results exposed the compounds drug character and DNA toxicity nature. The simulated results are given in Table-2.

TABLE-2
iGEMDOCK RESULTS AGAINST 1H9Z AND 3ZBO

Compound ID	Protein ID	Score in kcal/mol	Docking fitness
5BSFASB		-88.3	-83.95
a		-109.42	1364.3
b	1H9Z	-127.39	777.55
c	Radius in 12 Å	-122.22	572.81
d		-96.24	1203.76
e		-85.96	1014.00
5BSFASB		-69.62	18.19
a		-131.33	1377.00
b	3ZBO	-144.29	1370.00
c	Radius in 12 Å	-104.74	763.00
d		-143.29	1353.89
e		-106.16	1142.18

From the outcomes, this work revealed that the ligand binding ability is lower than the metal complexes. Docking results exposed that the ligand negative docking score such as -88.3, -69.62 kcal/mol. The series of complexes showed -109.42, -127.39, -122.22, -96.24, -85.96, -108.36 correspondingly for 1H9Z and -131.33, -144.29, -104.74, -143.29, -106.16, -136.67, respectively for 3ZBO. Apart from the six complexes, praseodymium complex exhibited higher binding ability against the proteins 1H9Z (-127.39) and 3ZBO (-144.29). Based on the docking results, all the synthesized molecules were carried for anti-microbial study. Some of the docking images are displayed in Figs. 4 and 5. The outcome images were processed through CLC drug discovery workbench-3 and visual studio softwares instead of autodock [29].

Antimicrobial activity: The biological inhibition experiments were conducted for determining antimicrobial activity of the compounds. Well diffusion method using 250 ppm in ethanol was filled and inhibited area was measured for each compound in millimeter (mm) after the incubated period. The outcomes of biocidal activities displayed (Fig. 6) that the zone of inhibition is higher for the praseodymium complex when compare to other metal(III) complexes. Inhibition zone of

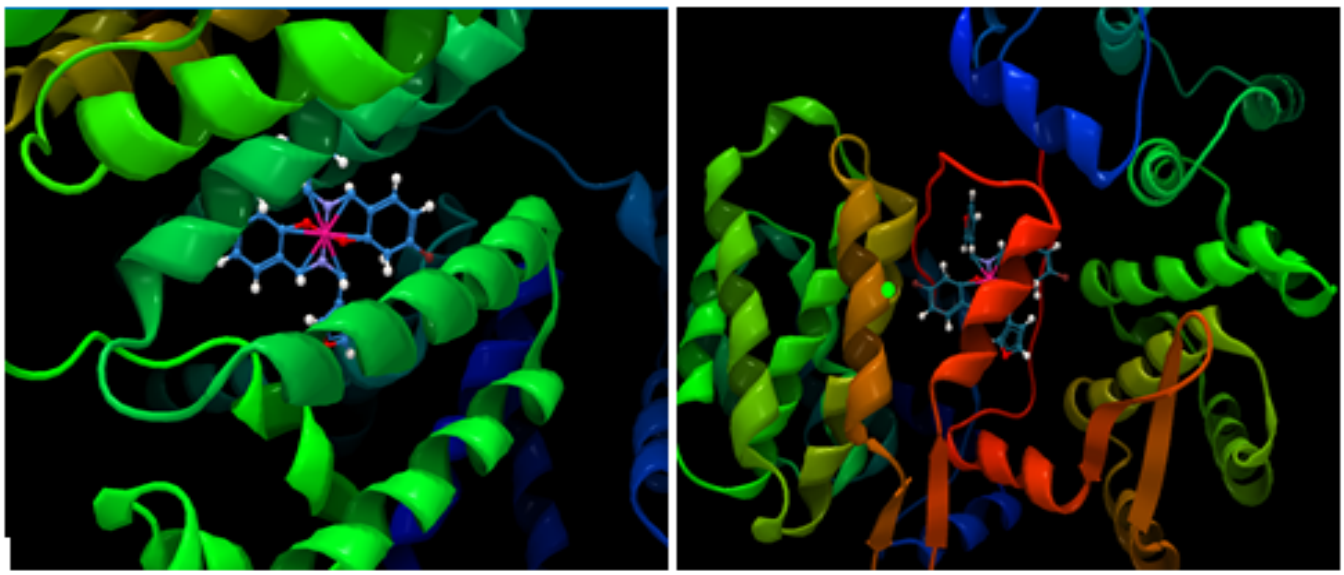

Fig. 4. Docking images against 1H9Z and 3ZBO of complex **b**

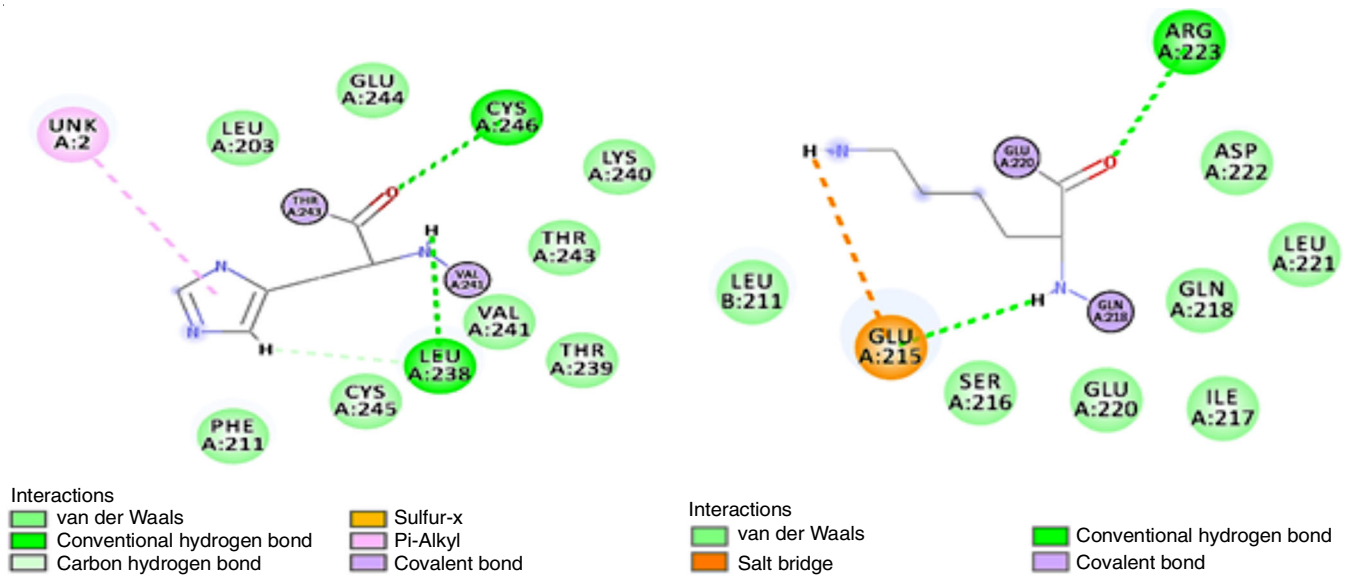

Fig. 5. 2D Docking images against 1H9Z and 3ZBO of complex **b**

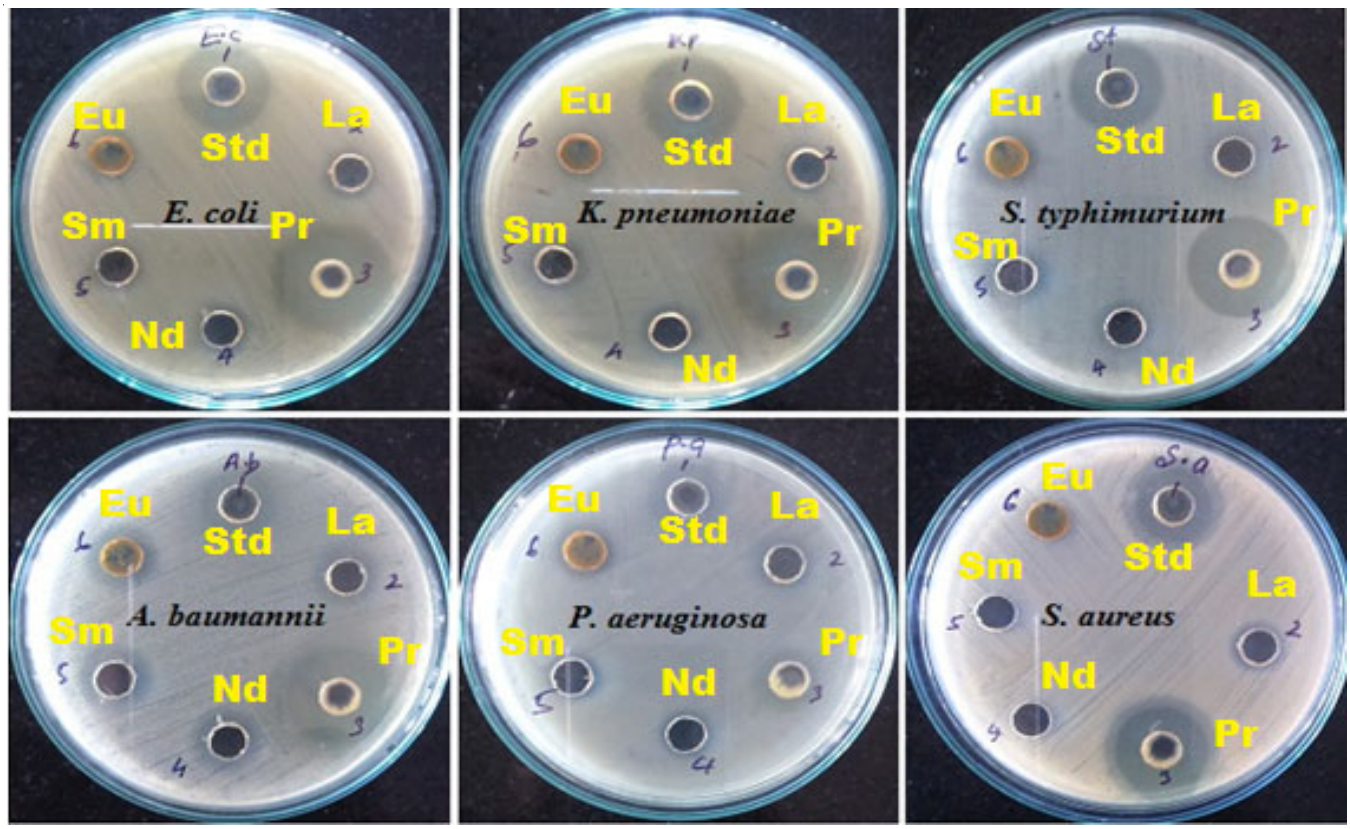

Fig. 6. Antimicrobial results of La, Pr, Nd, Sm and Eu (**a-e**) complexes

derivatives against the selected bacterial strains are presented in Table-3. This work revealed that the praseodymium complex exhibited the highest inhibition *viz*. 25, 25, 23, 23, 11 and 20 mm against all the studied pathogens. This work also identified that the inhibition of the complexes exist in the order of Pr > Gd > Eu > Nd > Sm > La complexes. However, all complexes exhibited lower inhibition against *P. aeruginosa*. Also, complex **b** exhibited good results than the standard gentamycin. These results almost coincidences with the reported values [30,31].

MTT assay and staining for praseodymium complex: Based on the docking and antimicrobial results, this work selected the praseodymium complex **b** for further anticancer activity against two cancer cell lines such as HeLa and MCF7 [32]. The influence of serially diluted concentrations such as 10, 25, 50, 100 and 250 µg/mL of complex **b** on selected cancer cell lines were investigated as per the reported protocol [33,34]. MTT assay carried on first human cancer HeLa cell line using complex **b** and the OD absorption results are displayed in

TABLE-3
ANTIMICROBIAL RESULTS FOR LIGAND AND COMPLEXES **a-e**

Compound ID	Zone of inhibition (mm) for 250 ppm					
	E. coli	*K. pneumoniae*	*S. typhimurium*	*A. baumannii*	*P. aeruginosa*	*S. aureus*
5BSFASB	17	20	15	16	8	16
a	15	15	14	14	–	12
b	25	25	23	23	11	20
c	21	20	20	22	–	18
d	18	20	17	18	–	15
e	20	20	20	15	10	18
Gentamicin	15	15	17	20	15	15
DMSO	–	–	–	–	–	–

Table-4. Similarly, Table-5 reported the percentage of cell viability of the colorimetric MTT assay. From the cell line results, 10 µg/mL concentrations exhibited the same like control absorption 0.38 ± 0.013 and the cell viability is also almost near value 82.87 ± 2.93 like control. Similar concentrations of complex **b** used on MCF7 cell line. When compared the direct action of cancer cells with complex **b**, MCF7 cells which has 40% transferrin supported inhibition of cell proliferation. Hence this study conducted the cell line study on breast cancer

TABLE-4
MTT ASSAY ABSORPTION
RESULTS OF **b** (Pr) WITH HeLa CELL

Conc. (µg/mL)	OD at 570 nm			Result
10	0.35	0.39	0.38	0.38 ± 0.013
25	0.30	0.29	0.29	0.29 ± 0.004
50	0.29	0.30	0.30	0.30 ± 0.003
100	0.26	0.25	0.27	0.27 ± 0.008
250	0.26	0.26	0.25	0.26 ± 0.005
Control	0.47	0.47	0.45	0.47 ± 0.010

TABLE-5
MTT ASSAY % OF CELL VIABILITY
RESULTS OF b (Pr) WITH HeLa CELL

Conc. (µg/mL)	Cell viability (%)			Result
10	75.80	82.87	80.51	82.87 ± 2.93
25	63.81	61.88	62.74	63.81 ± 0.79
50	62.53	64.24	63.60	64.24 ± 0.70
100	55.46	53.75	58.03	58.03 ± 1.75
250	55.67	54.82	52.89	55.67 ± 1.16
Control	100.40	99.60	99.21	100.00 ± 0.49

causing MCF7 cell line. The outcomes of OD at 570 nm and percentage of cell viability are displayed in Tables 6 and 7 respectively. From the results, all concentrations are almost controlling the cell growth from 10 to 250 µg/mL. But lower concentration 10 µg/mL showed highest OD and the deviation exists between 10 nm. In addition to the colorimetric outcomes, percentages of cell viability of both HeLa and MCF7 are shown in Figs. 7 and 8. These results revealed that praseodymium complex exposed good results such as OD for 10 µg/mL 0.594

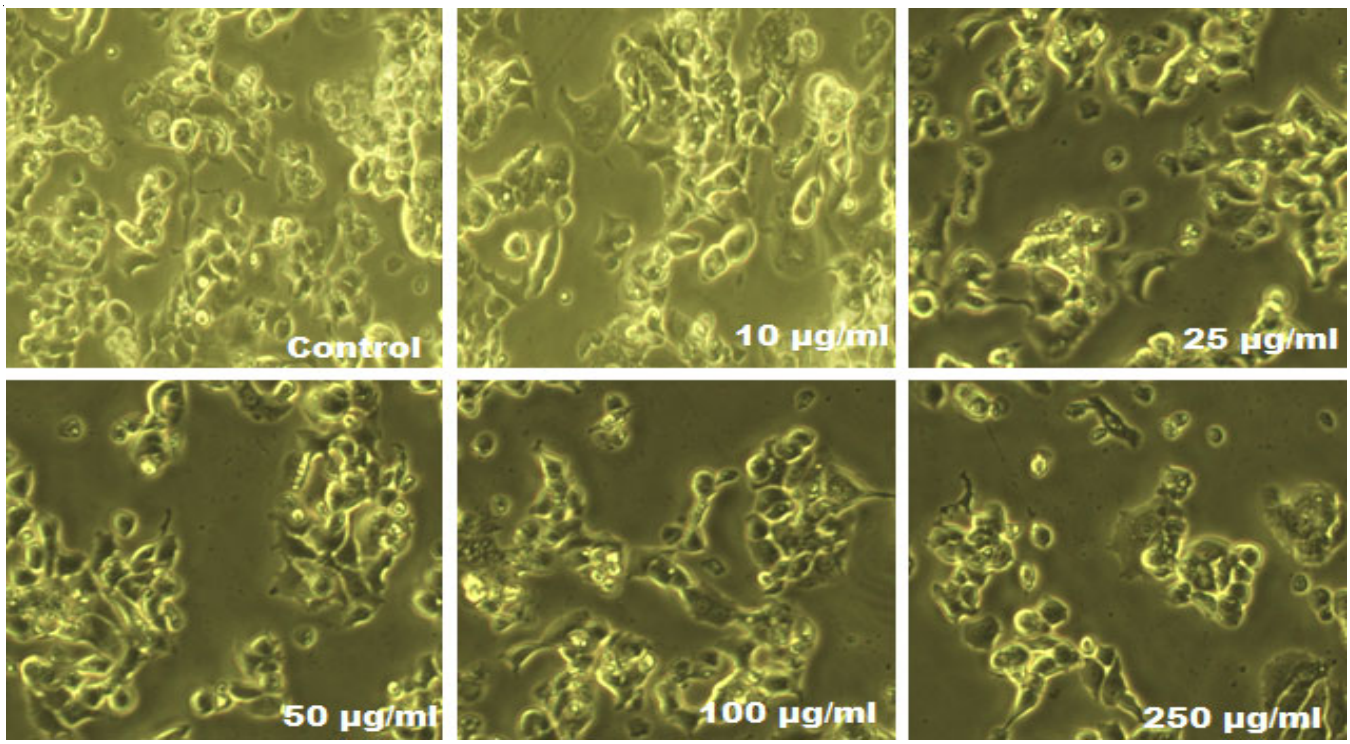

Fig. 7. MTT assay of Pr complex **b** with HeLa cell for different concentrations

TABLE-6
MTT ASSAY ABSORPTION
RESULTS OF **b** (Pr) WITH MCF7 CELL

Conc. (µg/mL)	OD at 570 nm (triplicate values)			Result
10	0.594	0.592	0.593	0.594 ± 0.0008
25	0.589	0.577	0.583	0.589 ± 0.0047
50	0.564	0.553	0.558	0.558 ± 0.0042
100	0.547	0.539	0.543	0.547 ± 0.0031
250	0.524	0.532	0.528	0.532 ± 0.0032
Control	0.598	0.604	0.601	0.604 ± 0.0024

TABLE-7
MTT ASSAY % OF CELL VIABILITY
RESULTS OF **b** (Pr) WITH MCF7 CELL

Conc. (µg/mL)	Cell viability (%) (triplicate values)			Result
10	98.835	98.502	98.668	98.668 ± 0.135
25	98.003	96.006	97.004	98.003 ± 0.815
50	93.843	92.013	92.928	93.843 ± 0.747
100	91.014	89.683	90.349	91.014 ± 0.543
250	87.188	88.519	87.853	88.519 ± 0.543
Control	100.00	100.00	100.00	100.00 ± 0.000

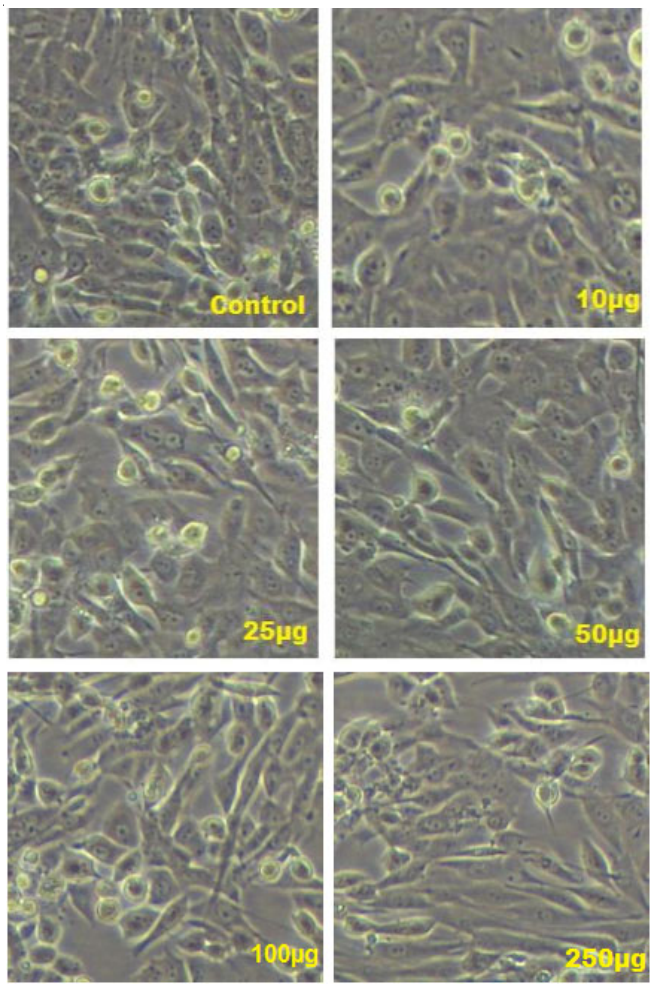

Fig. 8. MTT assay of Pr complex **b** with MCF7 cell for different concentrations

± 0.0008 and percentage cell viability 98.6689 ± 0.135, respectively in MCF7-MTT assay.

Conclusion

Few rare earth metal(III) complexes (M = Ln^{3+}, Pr^{3+}, Nd^{3+}, Sm^{3+} and Eu^{3+}) of Schiff base derived from 1-(furan-2-yl)-methanamine were synthesized and characterized. Theoretical docking and biological efficacy of the novel Schiff base ligand 5BSFASB and its metal(III) complexes (**a-e**) were completed to identify the multi-talented molecules. Initially, theoretical work completed for the synthesized molecules to avoid the wastage of chemicals, time and the microorganism. The theoretical docking exposed the binding ability of the compounds with drug transporting protein and the higher binding ability of the DNA glycosylases, which can be used to prove the activity of the prepared structure. Then the nature of the antimicrobial studies was conducted for the molecules and observed the good results for all the selected pathogens except *P. aeruginosa* when compare to gentamycin. These useful outcomes used to select the molecule for further anti-cancer investigation using praseodymium complex **b**. The MTT results on selected cancer cell line proved the efficiency and enhanced results of the selected complex when compare to the control molecule. Also this work identified the good control ability of the selected molecule. The results were coincidenced with the selected standards in each study. These chemo sensitivity *in vitro* assessment outcomes of *in vitro* calculation of the cytotoxic cancer cell lines specified that the cells were energetically flourishing when the period of compound administration. This work successfully measured the enhanced effects of praseodymium complex (**b**) in controlling the growth of disease causing pathogens and cancer-cell growth.

CONFLICT OF INTEREST

The authors declare that there is no conflict of interests regarding the publication of this article.

REFERENCES

1. H.-Q. Chang, L. Jia, J. Xu, T.-F. Zhu, Z.-Q. Xu, R.-H. Chen, T.-L. Ma, Y. Wang and W.-N. Wu, *J. Mol. Struct.*, **1106**, 366 (2016); https://doi.org/10.1016/j.molstruc.2015.11.001
2. F. Saraci, V. Quezada-Novoa, P.R. Donnarumma and A.J. Howarth, *Chem. Soc. Rev.*, **49**, 7949 (2020); https://doi.org/10.1039/D0CS00292E
3. M.T. Kaczmarek, M. Zabiszak, M. Nowak and R. Jastrzab, *Coord. Chem. Rev.*, **370**, 42 (2018); https://doi.org/10.1016/j.ccr.2018.05.012
4. V.A. Shelke, S.M. Jadhav, S.G. Shankarwar, A.S. Munde and T.K. Chondhekar, *Bull. Chem. Soc. Ethiop.*, **25**, 381 (2011); https://doi.org/10.4314/bcse.v25i3.68590
5. J. Huang, Y. Yang and C. Yuan, *Xibei Daxue Xuebao Ziran Kexueban*, **28**, 259 (1998).
6. P. Ghanghas, A. Choudhary, D. Kumar and K. Poonia, *Inorg. Chem. Commun.*, **130**, 108710 (2021); https://doi.org/10.1016/j.inoche.2021.108710
7. K. Mohanan, R. Aswathy, L.P. Nitha, N.E. Mathews and B.S. Kumari, *J. Rare Earths*, **32**, 379 (2014); https://doi.org/10.1016/S1002-0721(14)60081-8
8. A.K. Hijazi, Z.A. Taha, A.M. Ajlouni, W.M. Al-Momani, I.M. Idris and E.A. Hamra, *Med. Chem.*, **13**, 77 (2016); https://doi.org/10.2174/1573406412666160225155908
9. V. Balaram, *Geosci. Front.*, **10**, 1285 (2019); https://doi.org/10.1016/j.gsf.2018.12.005

10. D. Paul, G. Sanap, S. Shenoy, D. Kalyane, K. Kalia and R.K. Tekade, *Drug Discov. Today*, **26**, 80 (2021); https://doi.org/10.1016/j.drudis.2020.10.010
11. M.O. Steinhauser and S. Hiermaier, *Int. J. Mol. Sci*., **10**, 5135 (2009); https://doi.org/10.3390/ijms10125135
12. R. Singh, K. Sharma and R.V. Singh, *J. Sulfur Chem.*, **31**, 61 (2010); https://doi.org/10.1080/17415990903173529
13. A. Gupta, P. Gautam, K. Wennerberg and T. Aittokallio, *Commun. Biol.*, **3**, 42 (2020); https://doi.org/10.1038/s42003-020-0765-z
14. K.D. Thomas, A.V. Adhikari, I.H. Chowdhury, T. Sandeep, R. Mahmood, B. Bhattacharya and E. Sumesh, *Eur. J. Med. Chem.*, **46**, 4834 (2011); https://doi.org/10.1016/j.ejmech.2011.07.049
15. A. K. Hijazi, Z. A. Taha, A. M. Ajlouni, W. M. Al-Momani, I. M. Idris and E. A. Hamra, *J. Struct. Biol.*, **183**, 66 (2013); https://doi.org/10.1016/j.jsb.2013.04.007
16. I. Petitpas, A.A. Bhattacharya, S. Twine, M. East and S. Curry, *J. Biol. Chem.*, **276**, 22804 (2001); https://doi.org/10.1074/jbc.M100575200
17. R.H. Taha, Z.A. El-Shafiey, A.A. Salman, E.M. El-Fakharany and M.M. Mansour, *J. Mol. Struct.*, **1181**, 536 (2019); https://doi.org/10.1016/j.molstruc.2018.12.055
18. R.K. Dubey, U.K. Dubey and C.M. Mishra, *Indian J. Chem.*, **47A**, 1208 (2008).
19. P.B. Nariya, V.J. Shukla, N.R. Bhalodia and R.N. Acharya, *Ayu*, **32**, 585 (2011); https://doi.org/10.4103/0974-8520.96138
20. R.S. Joseyphus and M.S. Nair, *Mycobiology*, **36**, 93 (2008); https://doi.org/10.4489/MYCO.2008.36.2.093
21. R. Sukirtha, K.M. Priyanka, J.J. Antony, S. Kamalakkannan, R. Thangam, P. Gunasekaran, M. Krishnan and S. Achiraman, *Process Biochem.*, **47**, 273 (2012); https://doi.org/10.1016/j.procbio.2011.11.003
22. R.M. Issa, A.M. Khedr and H.F. Rizk, *Spectrochim. Acta A Mol. Biomol. Spectrosc.*, **62**, 621 (2005); https://doi.org/10.1016/j.saa.2005.01.026
23. L. Zapala, M. Kosinska, E. Woznicka, L. Byczynski and W. Zapala, *J. Therm. Anal. Calorim.*, **124**, 363 (2016); https://doi.org/10.1007/s10973-015-5120-0
24. M.J. Jisha and C.I. Sobana, *Int. J. Sci. Res. Pub.*, **7**, 10 (2017).
25. E. Pieniazek, J. Kalembkiewicz, M. Dranka and E. Woznicka, *J. Inorg. Biochem.*, **141**, 180 (2014); https://doi.org/10.1016/j.jinorgbio.2014.09.005
26. R.V. Singh, M. Pradeep, S. Ritu and S.P. Mital, *Am. Chem. Sci. J.*, **4**, 117 (2014); https://doi.org/10.9734/ACSJ/2014/6929
27. M. Hu, N. Li and K. Yao, *Front. Chem. China*, **1**, 369 (2006); https://doi.org/10.1007/s11458-006-0058-1
28. B.V. Sagar and H. Sriramula, *Iran. J. Chem. Chem. Eng*, **36**, 101 (2017).
29. A. Ramakrishnan, M. Renuka, V. Amalan, S. Senthilmurugan, N. Vijayakumar and S.J. Kim, *Trop. J. Pharm. Res.*, **19**, 1037 (2020); https://doi.org/10.4314/tjpr.v19i5.19
30. K.S. Abou-Melha and H. Faruk, *J. Coord. Chem.*, **61**, 1862 (2008); https://doi.org/10.1080/00958970701768455
31. I. Cota, V. Marturano and B. Tylkowski, *Coord. Chem. Rev.*, **396**, 49 (2019); https://doi.org/10.1016/j.ccr.2019.05.019
32. A.A. Palizban, A.H. Sadeghi and F. Abdollahpour, *Res. Pharm. Sci.*, **5**, 119 (2015).
33. J. Van Meerloo, G.J.L. Kaspers and J. Cloos, *Methods Mol. Biol*., 731 237 (2011); https://doi.org/10.1007/978-1-61779-080-5_20
34. P. Kumar, A. Nagarajan and P.D. Uchil, *Cold Spring Harb. Protoc.*, **6**, 469 (2018); https://doi.org/10.1101/pdb.prot095505